

Self-organizing height-arrow model: numerical and analytical results

Robert R. Shcherbakov*

*Bogoliubov Laboratory of Theoretical Physics, Joint Institute for Nuclear Research, 141980
Dubna, Russia.*

(October 3, 2018)

Abstract

The recently introduced self-organizing height-arrow (HA) model is numerically investigated on the square lattice and analytically on the Bethe lattice. The concentration of occupied sites and critical exponents of distributions of avalanches are evaluated for two slightly different versions of the model. The obtained exponents for distributions of avalanches by mass, area, duration and appropriate fractal dimensions are close to those for the BTW model, which suggests that the HA model belongs to the same universality class. For comparison, the concentration of occupied sites in the HA model is calculated exactly on the Bethe lattice of coordination number $q = 4$ as well.

PACS number(s): 05.70.Ln, 05.40.+j, 02.70.-c

Typeset using REVTeX

*On leave of absence from Theoretical Department, Yerevan Physics Institute, 375036 Yerevan, Armenia.

I. INTRODUCTION.

The study of different cellular automata, which exhibit Self-Organized Criticality (SOC) [1], has been a subject of great interest in recent years. These models serve as tractable limits of real dynamic systems with many spatial degrees of freedom, in which one might hope to gain understanding of possible mechanisms of SOC. Unfortunately, in most cases our current knowledge of the effects of SOC is rather limited.

The main peculiarity of the dynamic dissipative models which are self-driven into the SOC state is the presence of the power-law in distributions of quantities such as avalanche mass, duration, etc. These distributions are characterized by a set of exponents. One of the most intriguing questions concerns the classes of universality of these models. There are several attempts to shed light on this problem [2,3]. Recently, Ben-Hur and Biham [2] proposed a classification scheme for the $2d$ models both stochastic and deterministic. They found that the original Bak, Tang, Wiesenfeld (BTW) model [1] belongs to the universality class of *undirected* models, *directed* models form a separate class, and the two-state Manna model [4] belongs to the universality class of *random relaxation* models. Later on, Nakanishi and Sneppen [3] examined several $1d$ sandpile models and suggested that the two-state Manna model and rice pile model [5,6] belong to the same universality class.

This classification scheme is based on the type of relaxations at each site of the lattice. In the BTW model the particles from the toppled sites are uniformly redistributed among its nearest neighbors, whereas in the two-state Manna model the set of neighbors is chosen randomly. It is possible to introduce more complicated dynamical rules of relaxations at each site of the lattice that will depend on some period T where T is the number of topplings. During this period after each toppling the redistributions of particles from the given site form a minimal nonperiodic sequence. The BTW model can be considered with the period $T = 1$. In the two-state Manna model the sequence of topplings at each site is stochastic without any periodicity, therefore, one can put $T = \infty$ for this model.

In this paper, we investigate the recently introduced self-organizing height-arrow (HA) model [7,8]. It combines features of the BTW model [9,10] and self-organizing Eulerian walkers model (EWM) [7,11]. The model is a cellular automaton defined on any connected undirected graph. In this model, each site of the graph can be occupied by a particle or can be empty. Addition of the particle to the occupied site makes it unstable and causes its toppling. The site becomes empty and the particles are transferred to the nearest neighbors. The redistribution of particles from an unstable site is governed by the second site variable, *an arrow*. Each outgoing particle from the toppled site turns the arrow by the prescribed rule and the new direction of the arrow determines the destination point for this particle.

In the HA model T is formed by the nonperiodic sequence of turns of the arrow at each site of the lattice. For simplicity, it is convenient to assign the same period T for all sites of the lattice. Thus, one can define the HA model with increasingly complicated dynamical rules. These pseudo-random models tend to the random ones for large $T \rightarrow \infty$.

The goal of the paper is the study of the HA model with $T = 2$, when two topplings restore initial direction of the arrow. The model evolves at long times into the steady state which is identified with the SOC state as distributions of dynamic characteristics of the model show a power-law behavior. The obtained exponents for two slightly different types of this model are very close to those for the BTW one, which suggests that the HA model is

in the universality class of *undirected* models. We also study the main static characteristic of the model, the time averaged density of occupied sites. This quantity is obtained numerically on the square lattice and exactly on the Bethe lattice of coordination number $q = 4$.

The paper is organized as follows. The definition of the model with two slightly different types of evolution rules is presented in the next section. Sec. III is devoted to the numerical investigation of the HA model on the square lattice. Extrapolating results from finite size lattices we estimate the concentration of occupied sites in the model. The critical power-law exponents and scaling relations among them are defined in the framework of finite-size scaling analysis. We present results for the values of these exponents in the SOC state for distributions of various quantities of the HA model. Then, in Sec. IV, we exactly calculate the concentration of occupied sites on the Bethe lattice of coordination number $q = 4$. Discussion and conclusions are presented in Sec. V.

II. THE SELF-ORGANIZING HEIGHT-ARROW MODEL ON THE SQUARE LATTICE.

The HA model we are going to investigate is defined as follows. To each site i of the two-dimensional $L \times L$ square lattice is assigned a height variable $z_i \in \{0, 1, \dots\}$ and an arrow directed north, east, south or west from i . We start with an arbitrary initial configuration of heights and arrows on the lattice. Initially, we drop a particle on the randomly chosen site i . The succeeding evolution of the system is determined by the following rules. We increase the height variable at the site i by 1, $z_i \rightarrow z_i + 1$. If the site i is already occupied by the particle, it topples ($z_i \rightarrow z_i - 2$). To redistribute the particles from the toppled site i among its nearest neighbors, we turn the arrow twice according to the prescribed rules. For the given period $T = 2$, there are only two non-equivalent sequences of turns of the arrow at the given site which preserve the model from being directed. Hereafter, these sequences of turns will be distinguished as N-E-S-W-N and N-S-W-E-N. After each turn the new direction of the arrow points to the neighbor sites to which we will transfer particles at the next time step. This process continues until a stable configuration is reached. The sequence of topplings of unstable sites forms *an avalanche* which propagates through the lattice. After an avalanche ceases, we go on by adding a new particle and so on.

A given configuration of the model is a set of directions of arrows and heights. The total number of them is $8^{L \times L}$. During the evolution of the system the arrow at any site might be only in two positions due to the fact that the two subsequent topplings of the site restore the initial position of the arrow. Therefore, the set of configurations of the model falls into $2^{L \times L}$ equivalent classes which are determined by initial configurations of arrows.

Starting from a certain configuration of arrows and an arbitrary configuration of occupied sites, the model evolves through transient states into a dynamic attractor which is critical. This attractor is identified with the SOC state as different dynamic characteristics of the model show power-law tails in their distributions. The model being in the SOC state passes from one allowed stable configuration to another by avalanche dynamics. This critical state has been investigated in detail by Prietzhev [8]. He defined operators corresponding to addition of a particle at a randomly chosen site and showed that they commute with each other. The algebra of these operators is used to calculate the number of allowed configurations of a given class in the SOC state. This number is shown to be equal to the determinant of the

discrete Laplacian matrix Δ of the square lattice. To check the given configuration to be allowed in the SOC state the modification of the burning algorithm was also introduced [8].

III. NUMERICAL RESULTS.

In order to investigate the static properties and avalanche dynamics in the HA model, we have made numerical simulations with high statistics. We consider square lattices of size $L \times L$ with open boundary condition and L ranging from 100 up to 600. The HA model has been studied for two different types of dynamics (N-E-S-W-N and N-S-W-E-N) of turns of arrows and various initial conditions.

Starting from an arbitrary distribution of occupied sites and certain initial directions of arrows, the finite system evolves into a stationary state. In this state we have measured the time averaged density $\langle p(z = 1) \rangle$ and critical exponents for distributions of avalanches by mass (s), area (a) and duration (t). The mass s is defined as a total number of topplings in an avalanche whereas the area a is defined as a number of distinct sites visited by an avalanche. The simultaneous topplings of different sites in an avalanche at a given time is considered a single time step. The duration t is the number of this type of steps. For a more detailed description of the structure of an avalanche it is also useful to define a linear extent (diameter) of the avalanche cluster via a radius of gyration (r). We also measured the corresponding fractal dimensions γ_{xy} , where $x, y = \{s, a, t, r\}$.

As is shown in Fig. 1, the steady state is reached by the model after about 100 000 avalanches on the square lattice of the linear size $L = 600$ for the system which is initially empty and with a random initial distribution of arrows. In this simulation, we were recording the averaged density $\langle p(z = 1) \rangle$ of occupied sites at each time when the avalanche ceases.

As has been mentioned in Sec. II, the number of configurations of the model falls into $2^{L \times L}$ classes depending on the initial configurations of arrows. In our simulations of the HA model with the N-E-S-W-N dynamics we started from random initial configurations of arrows. Whereas, for the N-S-W-E-N dynamics the arrows were initially directed only east or south. The later case was chosen to simulate the scattering of particles at each toppling by 180° angle.

Fig. 2 displays the results of simulations for the time averaged density $\langle p(z = 1) \rangle$ in the stationary state. They slightly depend on the lattice size L and are well described by the equation $\langle p(z = 1) \rangle_L = p_c + cL^{-1}$. The numerical extrapolation of the $L \rightarrow \infty$ limit gives the values for the averaged density: $p_c \equiv \lim_{L \rightarrow \infty} \langle p(z = 1) \rangle_L = 0.721 \pm 0.001$ (N-E-S-W-N dynamics) and $p_c = 0.755 \pm 0.001$ (N-S-W-E-N dynamics). These values are a little higher in comparison with the stochastic two-state Manna model [4] (see Table I).

The form of avalanches in the HA model has a layered structure. A typical avalanche is shown in Fig. 3 where the number of relaxations in each site is marked by different scales of gray color. The sites with the same number of relaxations form a *layer* or *shell*. We have observed that layers group in pairs. In each pair a larger layer is a connected cluster with holes whereas a smaller one is a disconnected cluster without holes. Therefore, in the avalanche cluster there are a very few holes only near the surface in the first layer where each site topples once.

In Figs. 4, we present the directly measured distributions of avalanches by mass s , area a and duration t in a double logarithmic plot for the N-E-S-W-N dynamics and the lattice of

size $L = 600$. These distributions display a power-law behavior up to a certain cutoff which depends on the system size L . Since our simulations are limited by the lattices of finite size we ought to apply the finite-size scaling analysis [12,13] assuming the distribution functions scale with the lattice size L

$$P(x, L) = L^{-\beta_x} f_x(x \cdot L^{-\nu_x}), \quad (3.1)$$

where $f_x(xL^{-\nu_x})$ is a universal scaling function, x stands for s, a, t or r , and β_x and ν_x are critical exponents which describe the scaling of the distribution function. The finite-size scaling ansatz (3.1) can be rewritten in the following form [14]:

$$P(x, L) = x^{-\beta_x/\nu_x} \tilde{f}_x(x \cdot L^{-\nu_x}). \quad (3.2)$$

Let us suppose that distribution functions in the thermodynamic limit ($L \rightarrow \infty$) show pure power-law behavior for large enough stochastic variables (s, a, t, r)

$$P(x) \sim x^{-\tau_x}, \quad x \gg 1, \quad (3.3)$$

where $\tau_x, x \in \{s, a, t, r\}$ are critical exponents. This conjecture is mainly supported by computer simulations and different heuristic arguments [14]. Therefore, comparing (3.2) and (3.3) we get *the scaling relations* among these exponents

$$\tau_x = \frac{\beta_x}{\nu_x}. \quad (3.4)$$

From the fact that $\langle s \rangle \sim L^2$ in the undirected BTW-type models [9], one can get an additional scaling relation [14]

$$\nu_s(2 - \tau_s) = 2. \quad (3.5)$$

If we also assume that the stochastic variables s, a, t, r scale against each other, the appropriate fractal dimensions γ_{xy} can be defined via the following relations [15]:

$$\begin{aligned} s &\sim a^{\gamma_{sa}}, & a &\sim t^{\gamma_{at}}, \\ s &\sim t^{\gamma_{st}}, & a &\sim r^{\gamma_{ar}}, \\ s &\sim r^{\gamma_{sr}}, & t &\sim r^{\gamma_{tr}}, \end{aligned} \quad (3.6)$$

where $\gamma_{xy} = \gamma_{yx}^{-1}$. The set of exponents $\{\tau_x, \gamma_{xy}\}$ are not independent and scaling relations have the form [15,14]

$$\tau_x = 1 + \frac{\tau_y - 1}{\gamma_{xy}}. \quad (3.7)$$

From (3.7) one can find the simple expressions

$$\gamma_{xy} = \gamma_{xz}\gamma_{zy}. \quad (3.8)$$

We have 10 unknown exponents altogether, namely τ_x and $\gamma_{xy} = \gamma_{yx}^{-1}$, where $x, y \in \{a, s, t, r\}$, but there exists only 6 linearly independent scaling relations (3.7) among them. Additional scaling relations can be obtained from the specific structure and evolution of an avalanche

and depend on the given model. The compactness of an avalanche cluster gives us $\gamma_{ar} = 2$ [16,14].

Thus, estimating only three critical exponents from the numerical data, we can calculate all the others using the scaling relations Eqs. (3.7). Having calculated more than three exponents we are able to check these relations as well. The accurate determination of the τ 's exponents is a more difficult task than the γ 's due to the strict dependence of the τ 's on the system size L .

To reduce the fluctuations of the data, we integrated each distribution over bin lengths. The exponents γ_{xy} , $x, y = \{s, a, t\}$, are measured from the slopes of the straight parts of the corresponding graphs (Figs. 5). The obtained values are shown in Table II.

Plotting integrated distributions $P(t, L) \cdot L^{\beta_t}$ versus $t \cdot L^{-\nu_t}$ on a double logarithmic scale, as is shown in Fig. 6 for different lattice sizes L , we obtained from finite-size scaling analysis that the best data collapse corresponds to $\beta_t = 1.78 \pm 0.05$, $\nu_t = 1.36 \pm 0.05$ (Fig. 7). The scaling relation for the critical exponents (3.4) gives the value $\tau_t = 1.31 \pm 0.05$.

Next, we use the measured values of τ_t , γ_{st} and γ_{sa} to estimate the whole set of exponents using the scaling relations, Eqs. (3.7). These values are presented in Table II.

TABLES

TABLE I. The time averaged density p_c of occupied sites for the HA model on the square lattice with two slightly different types of dynamics and on the Bethe lattice is compared with the value for the two-state Manna model. The uncertainty of the numerical data is about ± 0.001 .

Density	Model			
	HA ^a	HA ^b	HA ^c	Manna [4]
p_c	0.721	0.755	$\frac{2}{3} \approx 0.666$	0.683

^aN-E-S-W-N dynamics

^bN-S-W-E-N dynamics

^cBethe lattice

TABLE II. The critical exponents for the $2d$ HA model evaluated in our work (first column) are compared with those for the BTW and two-state Manna models. The second column is the critical exponents for the BTW model obtained from numerical simulations, whereas in the third column we show exact values of the exponents for the BTW model based on the scaling relations (3.7), (3.8) and $\gamma_{sr} = \tau_r + 1$ [16]. Comparison of the critical exponents of the HA and BTW models evaluated from numerical simulations shows that the HA model belongs to the universality class of the BTW model. The uncertainty of the numerical data for the HA model is about ± 0.05 .

Exponent	Model			
	HA	BTW	BTW ^a	Manna
τ_s	1.18 ^b	1.20 [17]	$\frac{6}{5} = 1.2$ [19]	1.30 [4]
τ_a	1.21 ^b	1.22 [18]	$\frac{5}{4} = 1.25$ [19]	1.37 ^b
τ_t	1.31	1.32 [17]	$\frac{7}{5} = 1.4$ ^b	1.50 [4]
τ_r	1.41 ^b	1.42 ^b	$\frac{3}{2} = 1.5$ ^b	1.75 ^b
γ_{sa}	1.11	1.06 [2]	$\frac{5}{4} = 1.25$ ^b	1.23 [2]
γ_{st}	1.68	1.64 [17]	2 ^b	1.67 [4]
γ_{sr}	2.23 ^b	2.16 ^b	$\frac{5}{2} = 2.5$ ^b	2.49 ^b
γ_{at}	1.51	1.52 ^b	$\frac{8}{5} = 1.6$ ^b	1.35 [2]
γ_{ar}	2 ^c	2 ^c	2 ^c	2.01 ^b
γ_{tr}	1.33 ^b	1.32 [2]	$\frac{5}{4} = 1.25$ [16]	1.49 [2]

^aExact result.

^bThe value of the exponent is obtained from the scaling relations (3.7) and (3.8).

^cFrom the compactness of an avalanche cluster [16].

The simulations for the HA model with N-S-W-E-N dynamics within a small uncertainty give the same values for the critical exponents.

IV. THE HEIGHT-ARROW MODEL ON THE BETHE LATTICE.

In this section, we present exact analytical calculations for the averaged density of occupied sites in the HA model on the Bethe lattice of coordination number $q = 4$. The Bethe lattice is defined through a *Cayle tree* well-known in graph theory which is a connected graph with no closed circuits of edges. Then, the Bethe lattice is an infinite Cayle tree homogenous in the sense that all except the outer vertices have the same coordination number q [20].

Following Dhar [21], we approach the problem by dividing the allowed configurations of the HA model in the SOC state into two types: *strongly allowed* and *weakly allowed* and constructing the recurrent relations for the ratio of these configurations on the branches of the Bethe lattice. Using this ratio in the thermodynamic limit, we obtain the density of occupied sites in the HA model.

First, let us briefly describe the procedure of construction of the Cayle tree. Like many tree-like structures, the Cayle tree of k generations of coordination number q can be constructed by attaching q k th-generation branches to a central site, as is shown in Fig. 8. In turn, every k th-generation branch is constructed by connecting $q - 1$ ($k - 1$)th-generation branches to a new root and so on [20]. This property allows us to build recursion relations for the number of allowed configurations on the branches of the Cayle tree.

The number of boundary sites of the Cayle tree is comparable with interior ones. Hence, the calculation of the bulk properties in the thermodynamic limit requires special care. Since we are interested in the solution on the Bethe lattice, we will take the result for the averaged density of occupied sites calculated at the central site of the Cayle tree as the value for the Bethe lattice.

The definition of the HA model on this connected graph of coordination number $q = 4$ remains unchanged. The only difference from the square lattice concerns the notation of directions of arrows and sequences of their turns. We will consider only sequential clockwise turns by the right angle and denote the directions of arrows at each site simply by $\{1, 2, 3, 4\}$.

Let C be an allowed configuration on the k th-generation branch T_k with root vertex a . Adding a vertex b to T_k , one defines a subgraph $T' = T_k \cup b$. If the subconfiguration C' on T' with $z_b = 0$ and an arrow directed up or right (Fig. 9) becomes forbidden, C is called a *weakly allowed* (W) configuration, otherwise it is called a *strongly allowed* (S) one.

Now consider T_k with a root a that consists of three ($k - 1$)th-generation branches $T_{k-1}^{(1)}$, $T_{k-1}^{(2)}$ and $T_{k-1}^{(3)}$ with roots a_1 , a_2 and a_3 , respectively (Fig. 10). Let $N_W(T_k, n, \uparrow)$ and $N_S(T_k, n, \uparrow)$ be the numbers of distinct W- and S-type configurations on T_k with a given height $z_a = n$ and direction of the arrow at the root vertex a .

Let us also introduce

$$N_W(T_k) = \sum_{n=\{0,1\}} \sum_{r=\{\uparrow,\downarrow\}} N_W(T_k, n, r), \quad (4.1)$$

$$N_S(T_k) = \sum_{n=\{0,1\}} \sum_{r=\{\uparrow,\downarrow\}} N_S(T_k, n, r), \quad (4.2)$$

where the first summation is over the values of the heights and the second one is over the directions of the arrow. As has been already mentioned, the arrow at each site can take only two directions.

These numbers can be expressed in terms of the numbers of allowed subconfigurations on the three $(k-1)$ th-generation branches $T_{k-1}^{(1)}$, $T_{k-1}^{(2)}$ and $T_{k-1}^{(3)}$:

$$N_W(T_k) = N_S^{(1)} N_S^{(2)} N_S^{(3)} + N_S^{(1)} N_S^{(2)} N_W^{(3)} + N_S^{(1)} N_W^{(2)} N_S^{(3)} + N_S^{(1)} N_W^{(2)} N_W^{(3)} + N_W^{(1)} N_S^{(2)} N_S^{(3)} + N_W^{(1)} N_S^{(2)} N_W^{(3)} + N_W^{(1)} N_W^{(2)} N_S^{(3)} + N_W^{(1)} N_W^{(2)} N_W^{(3)}, \quad (4.3)$$

$$N_S(T_k) = 3N_S^{(1)} N_S^{(2)} N_S^{(3)} + 2N_S^{(1)} N_S^{(2)} N_W^{(3)} + 2N_S^{(1)} N_W^{(2)} N_S^{(3)} + N_S^{(1)} N_W^{(2)} N_W^{(3)} + 2N_W^{(1)} N_S^{(2)} N_S^{(3)} + N_W^{(1)} N_S^{(2)} N_W^{(3)} + N_W^{(1)} N_W^{(2)} N_S^{(3)}, \quad (4.4)$$

where $N_\alpha^{(i)} \equiv N_\alpha(T_{k-1}^{(i)})$, $\alpha = W, S$ and $i = 1, 2, 3$.

Let us define

$$X = \frac{N_W}{N_S}. \quad (4.5)$$

If we consider graphs $T_{k-1}^{(1)}$, $T_{k-1}^{(2)}$ and $T_{k-1}^{(3)}$ to be isomorphic, then $N(T_{k-1}^{(1)}) = N(T_{k-1}^{(2)}) = N(T_{k-1}^{(3)})$ and from (4.3) and (4.4) one obtains the following recursion relation:

$$X(T_k) = \frac{1}{3} (1 + X(T_{k-1})). \quad (4.6)$$

With the initial condition $X(T_0) = \frac{1}{3}$, this equation has a simple solution

$$X(T_k) = \frac{1}{2} - \frac{1}{2} 3^{-(k+1)}. \quad (4.7)$$

In the thermodynamic limit ($k \rightarrow \infty$) the iterative sequence $\{X(T_k)\}$ converges to a stable point $X^* = \frac{1}{2}$ that characterizes the ratio of the weakly allowed configurations to the strongly allowed ones in the SOC state.

Consider now a randomly chosen site O deep inside the Cayle tree (Fig. 11). The probability $P(1)$ of occupation of the site O is

$$P(1) = \frac{N(1)}{N_{\text{total}}}, \quad (4.8)$$

where $N(1)$ is the number of allowed configurations with $z = 1$ at the site O and $N_{\text{total}} = N(0) + N(1)$ is the total number of allowed configurations on the Cayle tree. The numbers $N(0)$ and $N(1)$ can be expressed via the numbers of allowed configurations on the four neighbor k th-generation branches $T_k^{(i)}$, $i = 1, 2, 3, 4$

$$N(0) = 2[1 + 2X + X^2] \prod_{i=1}^4 N_S(T_k^{(i)}), \quad (4.9)$$

$$N(1) = 2[1 + 4X + 5X^2 + 2X^3] \prod_{i=1}^4 N_S(T_k^{(i)}). \quad (4.10)$$

For the sites far from the surface in the thermodynamic limit ($k \rightarrow \infty$) we have $X = \frac{1}{2}$. Thus, from (4.9) and (4.10) we obtain

$$P(0) = \frac{1}{3}, \quad P(1) = \frac{2}{3}. \quad (4.11)$$

The value for the concentration of occupied sites $P(1)$ is in good qualitative agreement with the numerical result obtained on the square lattice.

V. CONCLUSION.

We numerically studied the self-organizing height-arrow (HA) model on the square lattice and analytically on the Bethe lattice. The dynamics of the model drives it into the critical attractor with spatio-temporal complexity. The obtained distributions of various dynamic characteristics show an explicit power law behavior which indicates long-range correlations in the steady state of the system. To obtain the critical exponents of distributions of dynamic quantities of the model in the SOC state, we applied the finite-size scaling analysis. The values of these exponents are listed in Table II and compared with known exponents of the BTW model and two-state Manna model. Thus, we argue that the HA model belongs to the universality class of undirected models.

Furthermore, we investigated the averaged density of occupied sites p_c in the SOC state of the HA model. It was also calculated exactly on the Bethe lattice of coordination number $q = 4$. The obtained results are presented in Table I.

ACKNOWLEDGMENTS

I would like to thank V.B. Priezzhev for valuable contributions and suggesting improvements. I thank N.S. Ananikian, E.V. Ivashkevich, D.V. Ktitarev, Vl.V. Papoyan, A.M. Polvolotsky and B. Tadic for fruitful discussions. Partial financial support by the Russian Foundation for Basic Research under grant No. 97-01-01030 is acknowledged.

REFERENCES

- [1] P. Bak, C. Tang, and K. Wiesenfeld, Phys. Rev. Lett. **59**, 381 (1987); Phys. Rev. A **38**, 364 (1988).
- [2] A. Ben-Hur and O. Biham, Phys. Rev. E **53**, R1317 (1996).
- [3] H. Nakanishi and K. Sneppen, Phys. Rev. E, (1997), to be published.
- [4] S.S. Manna, J. Phys. A: Math. Gen. **24**, L363 (1991).
- [5] K. Christensen, A. Correl, V. Frette, J. Feder, and T. Jøssang, Phys. Rev. Lett. **77**, 107 (1996).
- [6] M. Paczuski and S. Boettcher, Phys. Rev. Lett. **77**, 111 (1996).
- [7] V.B. Priezzhev, D. Dhar, A. Dhar and S. Krishnamurthy, Phys. Rev. Lett. **77**, 5079 (1996).
- [8] V.B. Priezzhev, (1997), to be published.
- [9] D. Dhar, Phys. Rev. Lett. **64**, 1613 (1990).
- [10] V.B. Priezzhev, J. Stat. Phys. **74**, 955 (1994).
- [11] R.R. Shcherbakov, V.I. Papoyan, and A.M. Povolotsky, Phys. Rev. E **55**, 3686 (1997).
- [12] L.P. Kadanoff, S.R. Nagel, L. Wu, and S. Zhou, Phys. Rev. A **39**, 6524 (1989).
- [13] M.N. Barber, in *Phase Transitions and Critical Phenomena*, edited by C. Domb and J.L. Lebowitz (Academic, London, 1983), Vol.8, p.144.
- [14] K. Christensen and Z. Olami, Phys. Rev. E **48**, 3361 (1993).
- [15] K. Christensen, H.C. Fogedby, and H.J. Jensen, J. Stat. Phys. **63**, 653 (1991).
- [16] S.N. Majumdar and D. Dhar, Physica A **185** 129 (1992).
- [17] S.S. Manna, Physica A **179**, 249 (1991).
- [18] S.S. Manna, J. Stat. Phys. **59**, 509 (1990).
- [19] V.B. Priezzhev, D.V. Ktitarev, E.V. Ivashkevich, Phys. Rev. Lett. **76**, 2093 (1996).
- [20] R.J. Baxter, *Exactly Solved Models in Statistical Mechanics*, (Academic Press, London, 1982).
- [21] D. Dhar and S.N. Majumdar, J. Phys. A: Math. Gen. **23** 4333 (1990).

FIGURES

FIG. 1. A computer simulation of the HA model (N-E-S-W-N dynamics) on the square lattice of the linear size $L = 600$ with open boundary conditions. The steady state is reached by the model after about 100 000 avalanches.

FIG. 2. The dependence of the time averaged density of occupied sites $\langle p(z = 1) \rangle_L$ on the lattice size L . (a) The HA model with N-E-S-W-N dynamics and random initial directions of arrows. (b) The same model with N-S-W-E-N dynamics and arrows initially directed east or south. The numerical extrapolation for the infinity lattice size $L \rightarrow \infty$ gives (a) $p_c = 0.721 \pm 0.001$ and (b) $p_c = 0.755 \pm 0.001$.

FIG. 3. A typical form of an avalanche cluster of the HA model. The lattice size is $L = 200$. The avalanche cluster has a layered structure. The number of topplings in each layer is indicated in gray scale.

FIG. 4. Simulation results for distributions of avalanches by (a) mass (b) area and (c) duration of the HA model in the SOC state. The linear size of the lattice is $L = 600$. The number of avalanches for each distribution is 10^7 .

FIG. 5. Double-logarithmic plot of the dependence of the stochastic variables $\{s, a, t\}$ against each other for different lattice sizes. The distributions are integrated over bin lengths.

FIG. 6. Double-logarithmic plot of the integrated distribution of avalanches $P(t, L)$ versus duration t for five lattice sizes $L = 100, 200, \dots, 500$. Each distribution is averaged over 10^7 avalanches.

FIG. 7. Finite-size scaling plot for the integrated distributions $P(t, L)$. The data for different L collapse onto a single curve for $\beta_t = 1.78$ and $\nu_t = 1.36$

FIG. 8. Construction of the Cayle tree with $q = 4$ and $k = 3$ generations by attaching $q = 4$ k th-generation branches to a central site. This procedure is explained in the text.

FIG. 9. A k th-generation branch T_k and vertex b form a subgraph T' . The ovals denote the rest of the subbranches of T_k .

FIG. 10. A k th-generation branch T_k consists of three nearest $(k - 1)$ th-generation branches $T_{k-1}^{(1)}$, $T_{k-1}^{(2)}$ and $T_{k-1}^{(3)}$.

FIG. 11. A site O with height $z_o = n$ and a given direction of the arrow is located deep inside the lattice and surrounded by the four k th-generation branches $T_k^{(1)}$, $T_k^{(2)}$, $T_k^{(3)}$ and $T_k^{(4)}$.

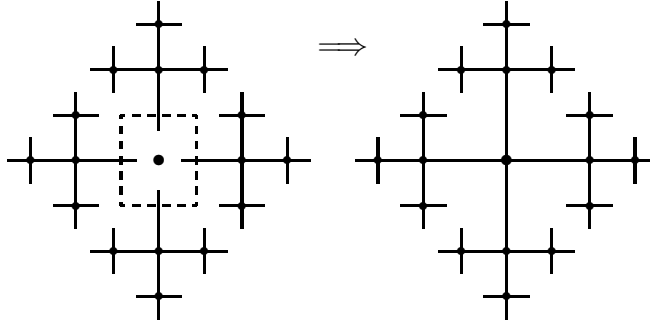


FIG. 8. Construction of the Cayley tree with $q = 4$ and $k = 3$ generations by attaching $q = 4$ k th-generation branches to a central site. This procedure is explained in the text.

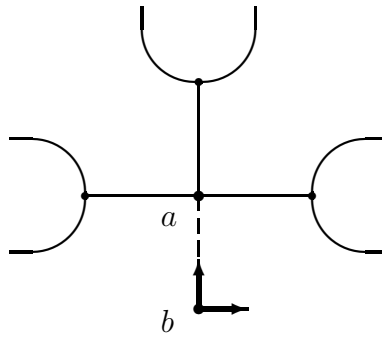


FIG. 9. A k th-generation branch T_k and vertex b form a subgraph T' . The ovals denote the rest of the subbranches of T_k .

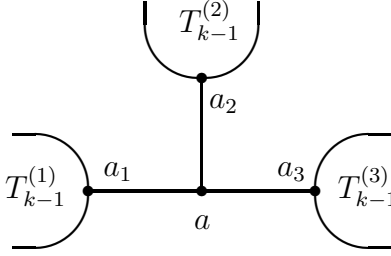


FIG. 10. A k th-generation branch T_k consists of three nearest $(k - 1)$ th-generation branches $T_{k-1}^{(1)}$, $T_{k-1}^{(2)}$ and $T_{k-1}^{(3)}$.

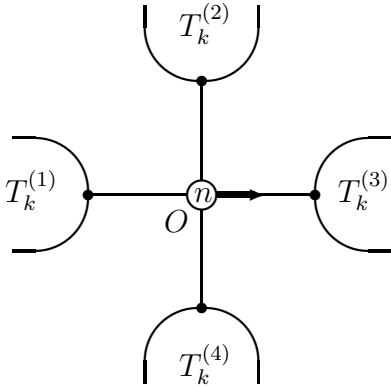


FIG. 11. A site O with height $z_o = n$ and a given direction of the arrow is located deep inside the lattice and surrounded by the four k th-generation branches $T_k^{(1)}$, $T_k^{(2)}$, $T_k^{(3)}$ and $T_k^{(4)}$.

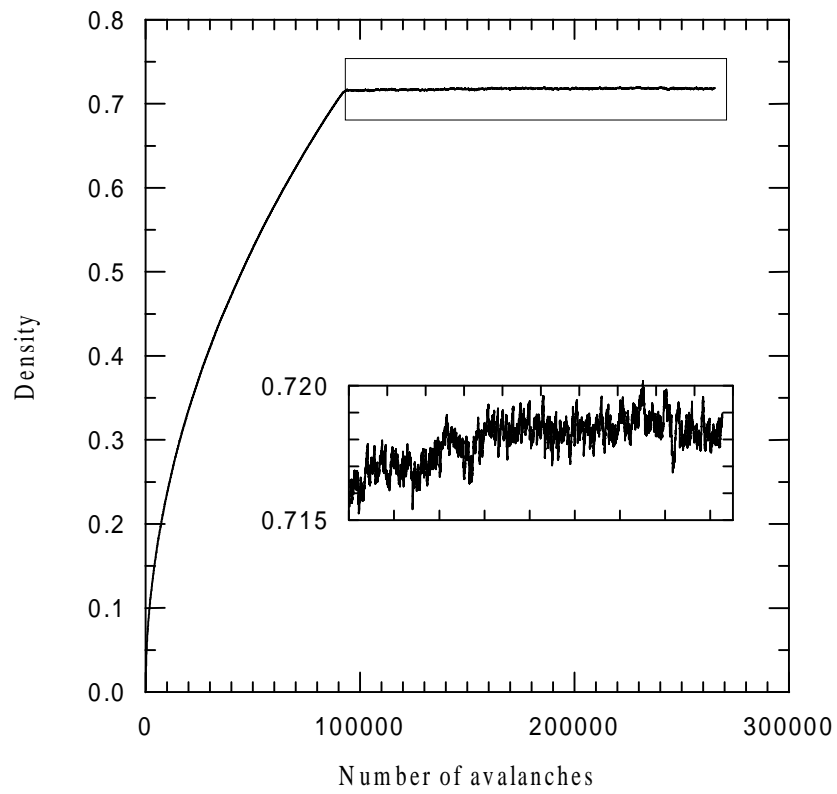


FIG. 1. A computer simulation of the HA model (N-E-S-W-N dynamics) on the square lattice of the linear size $L=600$ with open boundary conditions. The steady state is reached by the model after about 100000 avalanches.

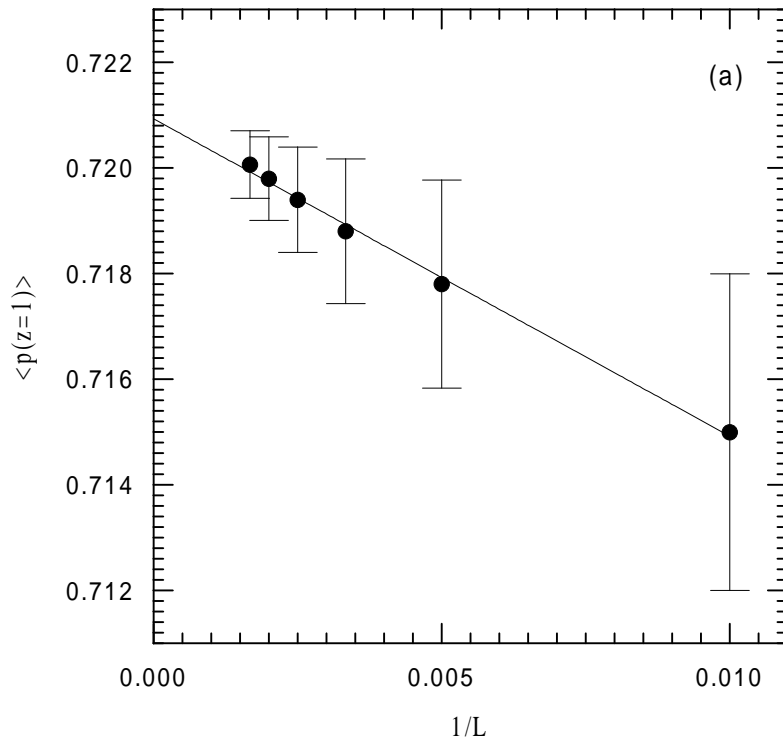


FIG. 2. The dependence of the time averaged density of occupied sites $\langle p(z=1) \rangle$ on the lattice size L . (a) The HA model with N-E-S-W-N dynamics and random initial directions of arrows. (b) The same model with N-S-W-E-N dynamics and arrows initially directed east or south. The numerical extrapolation for the infinity lattice size ($L \rightarrow \infty$) gives (a) $p_c = 0.721 \pm 0.001$ and (b) $p_c = 0.755 \pm 0.001$.

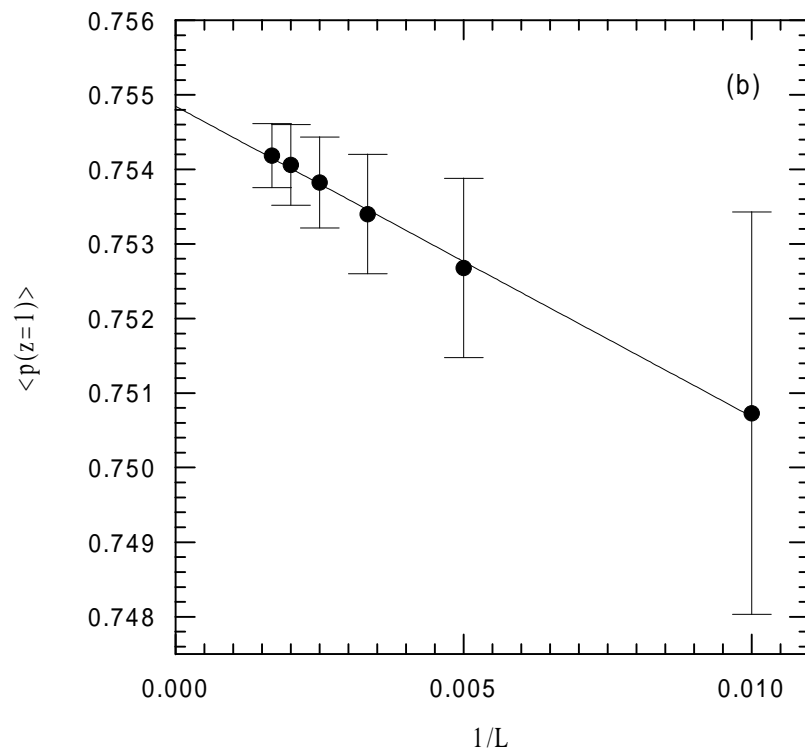


FIG. 2. (b)

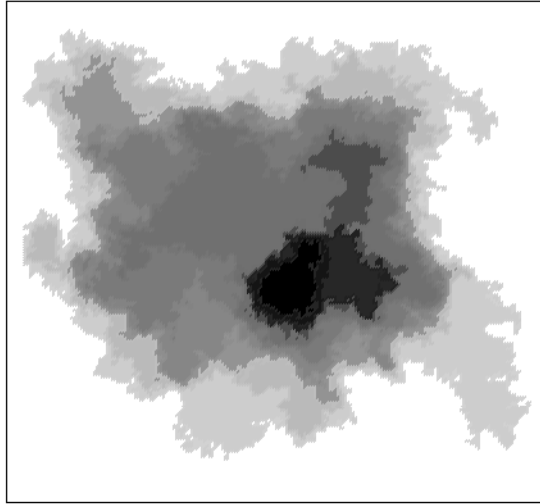


FIG. 3: A typical form of an avalanche cluster of the HA model. The lattice size is $L = 200$. The avalanche cluster has a layered structure. The number of topplings in each layer is indicated in gray scale.

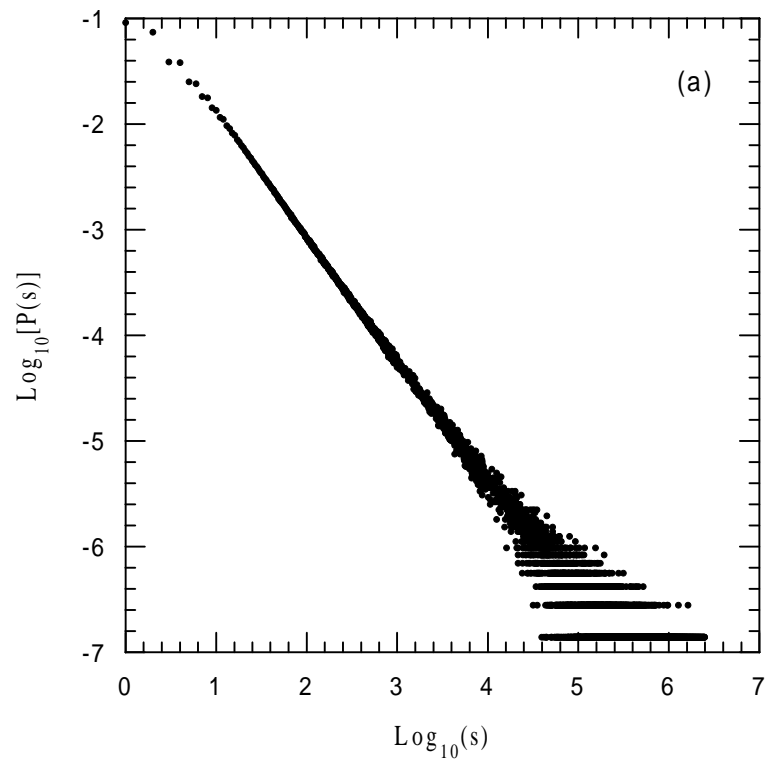


FIG. 4. Simulation results for distributions of avalanches by (a) mass, (b) area, and (c) duration of the HA model in the SOC state. The linear size of the lattice is $L=600$. The number of avalanches for each distribution is 10^7 .

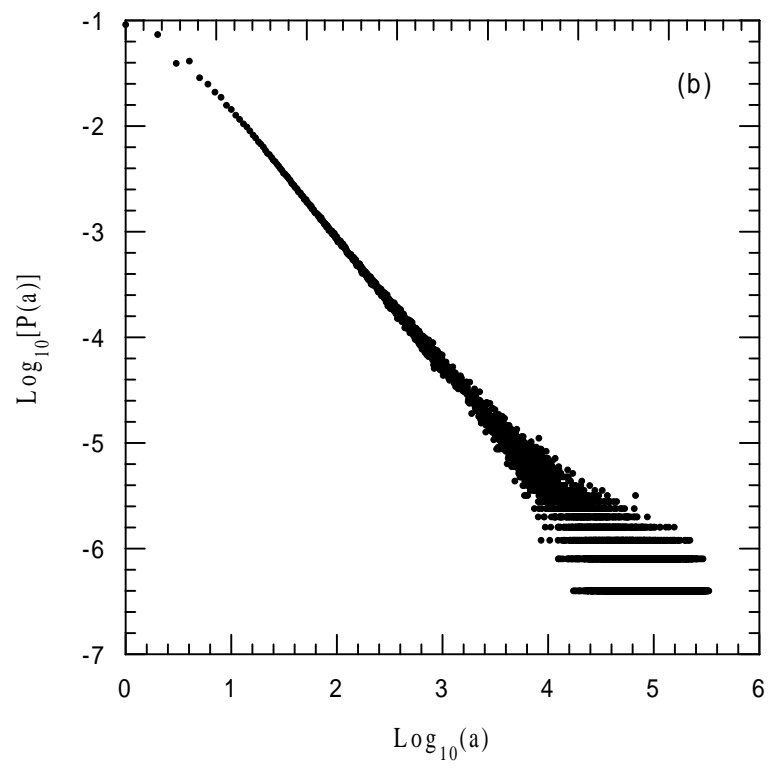


FIG. 4. (b).

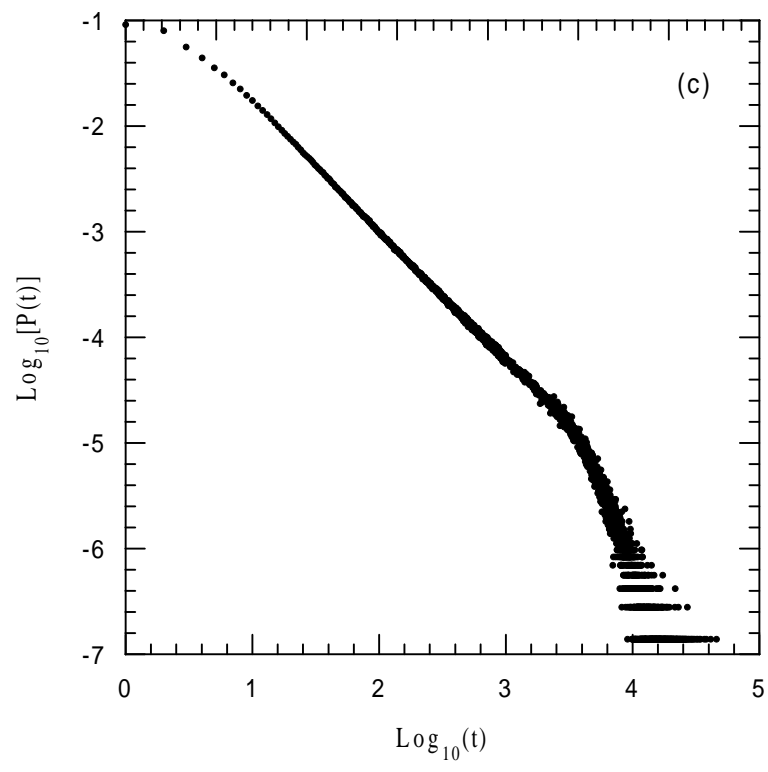


FIG. 4. (c).

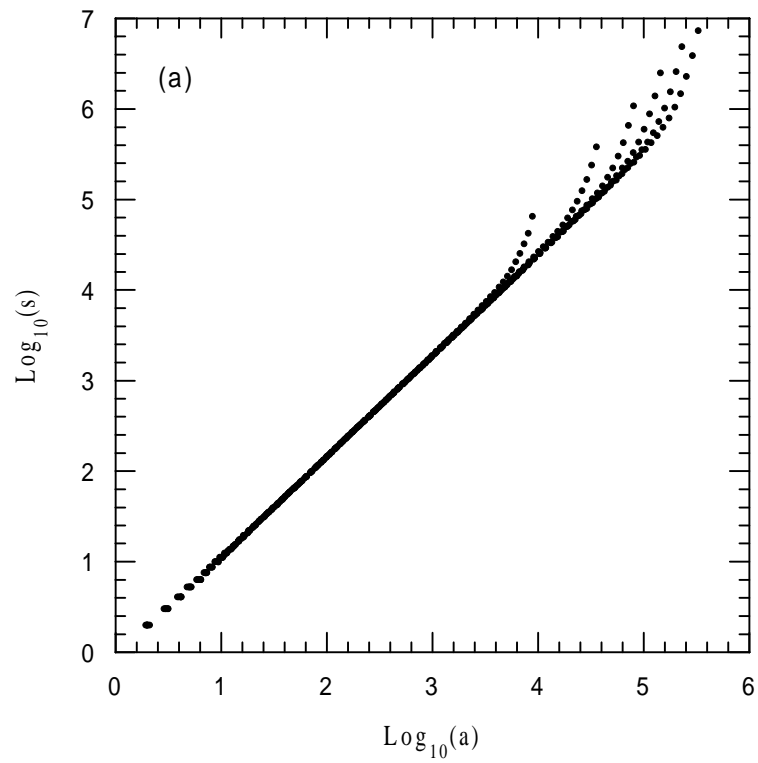


FIG. 5. Double-logarithmic plot of the dependence of the stochastic variables $\{s, a, t\}$ against each other for different lattice sizes. The distributions are integrated over bin lengths.

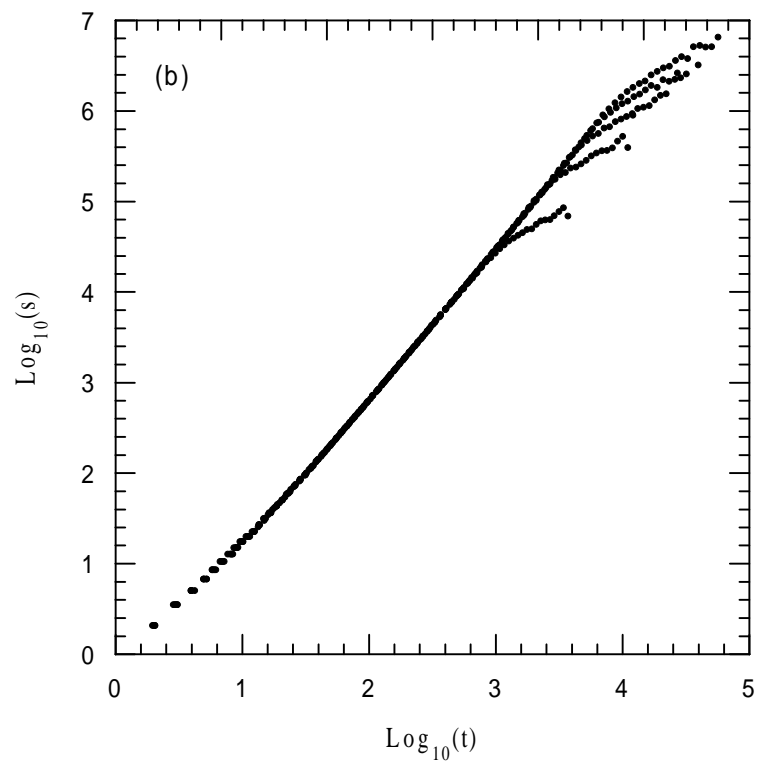


FIG. 5. (b)

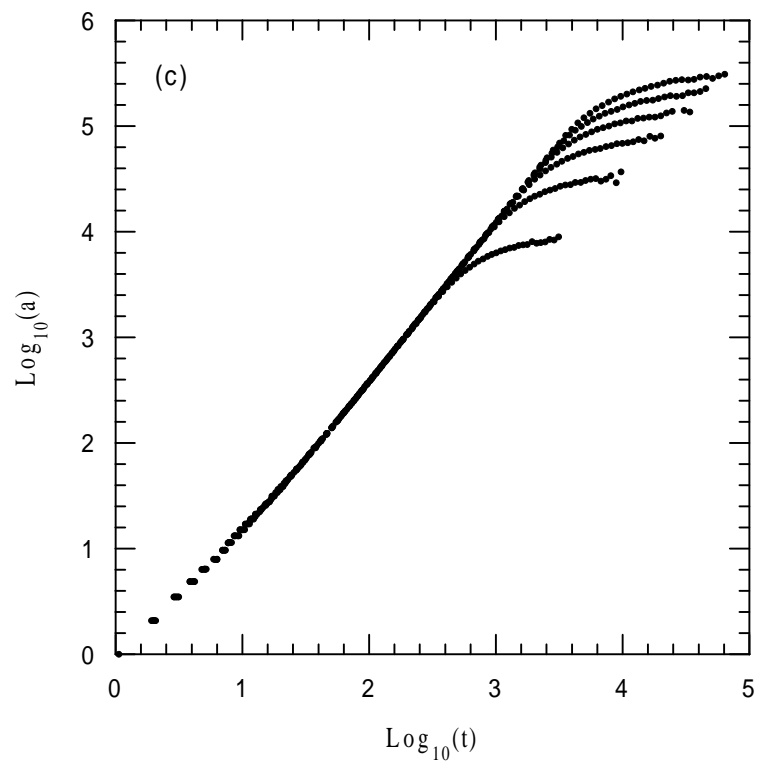


FIG. 5. (c)

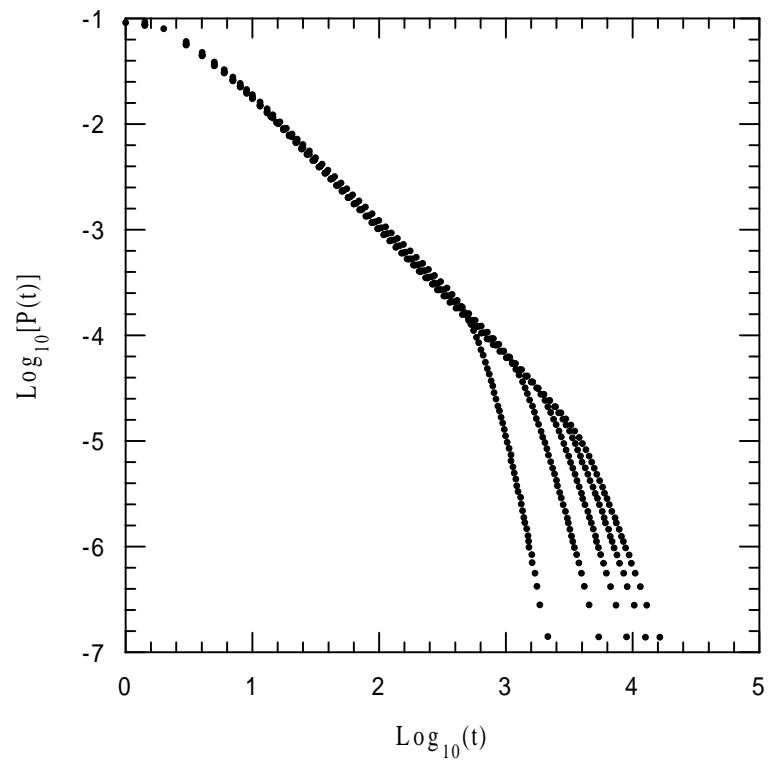


FIG. 6. Double-logarithmic plot of the integrated distribution of avalanches $P(t,L)$ versus duration t for the five lattice sizes $L=100, 200, \dots, 500$. Each distribution is averaged over 10^7 avalanches.

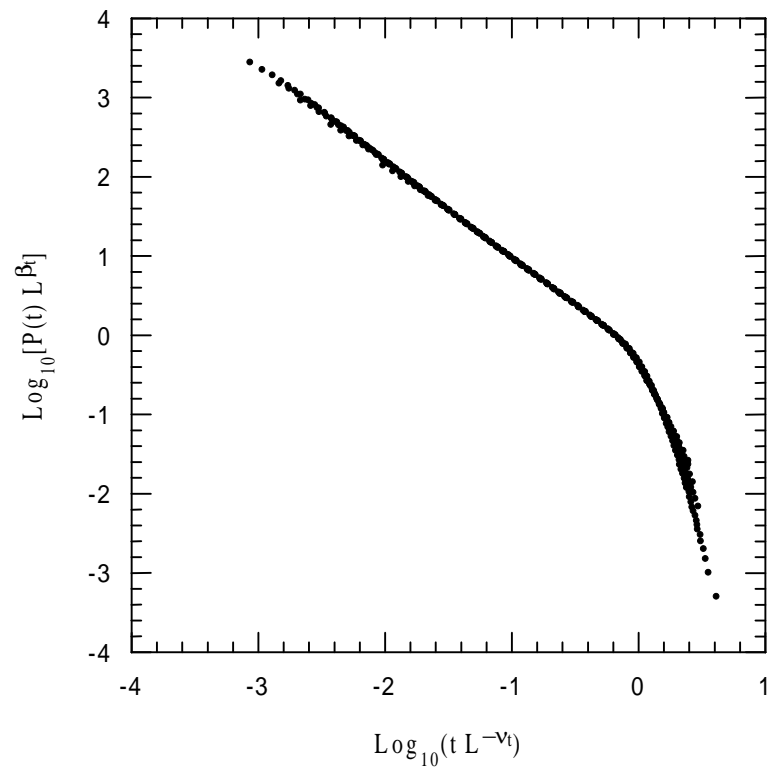


FIG. 7. Finite-size scaling plot for the integrated distributions $P(t,L)$. The data for different L collapse onto a single curve for $\beta_t = 1.78$ and $\nu_t = 1.36$.